On the calculation of cross-flooding time

Pekka Ruponen, Patrick Queutey, Marek Kraskowski, Risto Jalonen, Emmanuel Guilmineau

Ruponen et al. 2012. On the calculation of cross-flooding time, *Ocean Engineering* 40:27-39
doi:10.1016/j.oceaneng.2011.12.008 (accepted manuscript)

On the calculation of cross-flooding time

By Pekka Ruponen[1*], Patrick Queutey[2], Marek Kraskowski[3], Risto Jalonen[4], Emmanuel Guilmineau[5]

[1 *] (corresponding author) Napa Ltd., P.O. Box 470, FI-00181, Helsinki, email pekka.ruponen@napa.fi

[2] LMF, UMR 6598 CNRS, Ecole Centrale de Nantes, P.O. Box 92101, Nantes, France. email patrick.queutey@ec-nantes.fr

[3] Ship Design and Research Centre S.A., 65 Szczecinska St., 80-392 Gdansk, Poland., email marek.kraskowski@cto.gda.pl

[4] Marine Technology Group, Aalto University School of Engineering, P.O. Box 15300, FI-00076 Aalto, Finland, emailristo.jalonen@aalto.fi

[5] LMF, UMR 6598 CNRS, Ecole Centrale de Nantes, P.O. Box 92101, Nantes, France. Tel. +33 240371681, fax +33 240372523, email emmanuel.guilmineau@ec-nantes.fr

Abstract

Asymmetric flooding in a damaged ship is a dangerous situation. Cross-flooding ducts are used to provide the necessary equalization across the ship in order to decrease the heeling angle. The elapsed time for this passive counteraction depends on the arrangement of the ducts and the tanks. In addition the air pipes have a significant effect since air must be vented from the flooded tanks. This paper presents CFD calculations, applied to obtain the discharge coefficient of the whole cross-flooding duct, as well as for assessing the pressure losses for air flow in two typical air pipe designs. The results are combined in order to study their final effect on the time to equalize the asymmetric flooding. Calculations are performed by using both simplified approaches and time-domain simulation. The results indicate that small inaccuracies in the applied coefficients have only a minimal effect on the results. Thus the use of simplified methods for determination of the applied discharge coefficients seems to be justified. However, the use of CFD and time-domain simulations may be necessary for exceptional arrangements. The results also indicate that neither the scale 1:3 nor the inlet pressure height has significant effect on the discharge coefficient.

Keywords: *damage stability, cross-flooding, discharge coefficient, CFD, air compression, pressure loss, time-to-flood, validation*

1. Introduction

Damage stability is essential for ship safety. Flooding is often asymmetric and the consequent heeling may end either rapidly or more slowly in either a safe or a less safe state of the ship. In worst cases, the ship may capsize quickly. Therefore, requirements have been established regarding provisions for rapid counter flooding that will equalize the heeling. Stability during the transient stages of flooding is always better that at the final stage provided that the floodwater can uniformly spread over the entire compartment, *Pawlowski (2004)*. Thus cross-flooding is always beneficial, despite the increase of sinkage. This passive counter action is typically arranged through a pipe or a duct in the double bottom. For structural reasons there are usually girders and stiffeners in the duct, having some effect on the flow through the duct.

Another notable effect is the air compression in the undamaged side. As the floodwater flows through the cross-flooding device to the tank, the air must be removed through the ventilation pipes. Naturally, very large air pipes are not feasible since they restrict the general arrangement on the decks above the tank. Thus the challenge of the designer is to find the optimal cross-flooding and air pipe configuration that allows fast enough equalization of flooding in asymmetric damage cases but does not require too much space.

The requirement for the maximum time for equalization has recently been tightened from 15 min to 10 min. In addition, separate calculation of intermediate stages is required for passenger ships, if

sufficient equalization exceeds 60 seconds (*IMO, 2008*). These changes in the regulations have emphasized the need for further research on the calculation of cross-flooding time.

The simple calculation method for cross-flooding time, first presented by *Solda (1961),* was adopted as the IMO Resolution A.266 (VIII), *IMO (1973)*. Recently, this has been slightly revised and the current version is known as the IMO Resolution MSC.245(83), *IMO (2007)*. The principal idea has remained the same for half a century. During the latest revision only the interpretation of the pressure-loss coefficients (k_i) was slightly changed and the importance of air compression and ventilation level was included.

Recently, also time-domain flooding simulation tools have been applied to the calculation of cross-flooding times, *Peters et al. (2003)* and *Ruponen and Routi (2007)*. The major benefit is the possibility to take into account the ship motions during the cross-flooding in a realistic way. Also the real geometry of the flooded rooms and the compression of air due to a restricted ventilation level can be modelled.

Interestingly, *Solda (1961)* presented the simplified method as an alternative for calculation with "successive steps" that was considered to be too laborious at that time. Since then the calculation capacity of computers has increased significantly. Considering this, it is strange that the simplified approach is still the industry standard for assessment of cross-flooding times. *Vassalos (2009)* suggests that "the simplified time-domain simulation codes need to be supported, by using computational fluid dynamics (CFD) as the only viable option for proper treatment of the cross-flooding problem". However, no arguments for this conclusion are given. Therefore, a systematic study was carried out in order to compare the different methods for determination of the discharge coefficients and for the calculation of cross-flooding time. The presented case study concentrates on a single damage scenario that is calculated with different methods. The results are compared and the pros and cons of each method are discussed.

2. Previous research on determination of discharge coefficients

During the revision of the regulation for the assessment of the cross-flooding time (*IMO, 2007*) special attention was paid on the cross-ducts for the first time, and systematic CFD computations were carried out. The major outcome of the study was the regression formulae for the effective discharge coefficient of a cross-duct. The parameters are the distance between the girders and the number of manholes on the girders (*Pittaluga and Giannini, 2006*). The results indicate that the pressure losses in the duct decrease as the distance between the girders is shortened. However, structural stiffeners were not taken into account in the numerical model.

A systematic experimental study on determination of discharge coefficient for a cross-flooding duct in scale 1:3 pointed out the importance of structural stiffeners inside the duct *Stening et al. (2011)*. In the experiments the addition of the stiffeners increased the discharge coefficient of the duct by 7.5%. However, neither a web frame in the middle of the cross-duct nor small inclination angle of 7° had any notable effect on the discharge coefficient. Moreover, the experimentally obtained discharge coefficients for all variations of the duct design were significantly smaller than the values obtained from the regression equation, based on the previous CFD calculations (*Pittaluga and Giannini, 2006*).

Recently also NMRI in Japan has carried out model tests in scale 1:10 and performed comparative CFD calculations, *IMO (2010),* in order to validate the regression formulae, presented by *Pittaluga and Giannini (2006)*. Contrary to the results of *Stening et al. (2011),* both the initial experimental and CFD results slightly over-estimated the pressure losses in the duct. It is noteworthy that the stiffeners were not included in the NMRI study.

The present study comprises of dedicated CFD computations for determination of the discharge coefficient of a typical cross-duct design. The effects of both the scale and the inlet pressure height are analyzed. In addition CFD is used to assess pressure losses in two typical air pipe configurations. Finally, a systematic comparison of time-domain flooding simulation and the simplified method is

carried out. The cross-flooding times are calculated with both methods by using the discharge coefficients that are determined with different methods.

3. IMO Resolution MSC.245(83)

3.1. Background

Previously known as the Resolution A.266 (VIII), *IMO (1973)*, the regulation has been recently updated, *IMO (2007)*. However, the basic concept and equations have remained the same. Most notably, the effect of counter air pressure was included in the rule. This needs to be taken into account if the area of the air pipes is less than 10 % of the effective area of the cross-flooding ducts.

The resolution allows four alternative methods for assessing the equalization time:

- Simplified formula, *Solda (1961)*
- Computational fluid dynamics (CFD)
- Time-domain flooding simulation
- Model tests

CFD tools can be used with two different ways: either only for evaluation of the effective discharge coefficient of the duct or for calculation of the cross-flooding time. In the latter case the CFD solver should be coupled with the simulation of the ship motions during the flooding.

In the present research, all of these alternative methods are utilized in a comprehensive case study. The primary objective is to assess the effect of different methods and small variations in the applied data on the equalization time. In the following, the under-lying physics and assumptions of the simplified formula are presented and discussed.

3.2. Simplified approach

The simplified method for assessing the cross-flooding time is exactly the same as the original one, presented by *Solda (1961)*. In principle, this is limited to flooding through only a single flooding device. Some simplified methods for accounting successive openings and parallel cross-ducts have also been presented, *IMO (2007)*.

The time required from commencement of cross-flooding to the final equilibrium heeling angle is estimated with the following formula:

$$T_f = \frac{2W_f}{S \cdot F} \cdot \frac{\left(1 - \sqrt{\frac{h_f}{H_0}}\right)}{\sqrt{2gH_0}} \cdot \frac{1}{\left(1 - \frac{h_f}{H_0}\right)}, \tag{1}$$

where W_f is the volume of water that must flow through the equalization device (opening, pipe or duct), S is the effective cross-section area of the device, g is the acceleration due to gravity, H_0 is the head of water before commencement of cross-flooding and h_f is the head of water after cross-flooding.

The "dimensionless factor of reduction of speed through the equalization device" is the effective discharge coefficient for the whole duct:

$$F \equiv C_{d,eff} \tag{2}$$

The applied pressure heads and the basic definitions are illustrated in Fig. 1. The damaged rooms and the cross-duct (dark shaded area) are considered to be instantly flooded (open to sea), thus creating the asymmetric flooding condition. At the time $t = 0$ the equalizing flooding through the cross-duct starts.

The Eq. (1) is based on the assumption that the decrease of the heel angle and the effective pressure head on the duct outlet are directly proportional to the volume of floodwater in the tank on the undamaged side, *Solda (1961)*. In principle, this is fully valid only to rooms with perpendicular walls and only at small heel and trim angles.

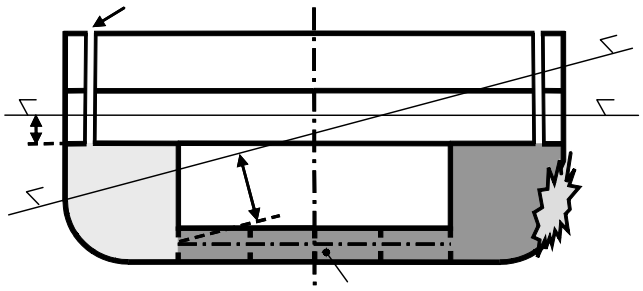

Fig. 1. Definitions for cross-flooding, the dark shaded area is considered to be instantly flooded.

3.3. Discharge coefficients

Both the simplified method in the IMO Resolution MSC.245(83) and time-domain flooding simulation, e.g. *Ruponen (2007)*, are based on the hydraulic model. For a streamline from point A in the damaged tank to point B in the outlet of the cross-duct, Bernoulli's equation can be written as:

$$\int_A^B \frac{dp}{\rho} + \frac{1}{2}\left(u_B^2 - u_A^2\right) + g(h_B - h_A) + \frac{1}{2}k_L u_B^2 = 0\,, \tag{3}$$

where p is air pressure, u is flow velocity and h is the water height from the common reference level. All losses in the duct are represented by the non-dimensional pressure-loss coefficient k_L. Consequently, by assuming that $p_A = p_B$ and $u_A = 0$, the volumetric flow through an opening with area dS is:

$$dQ = C_d \cdot \sqrt{2g(h_A - h_B)} \cdot dS\,, \tag{4}$$

where the discharge coefficient is:

$$C_d = \frac{1}{\sqrt{1 + k_L}} \tag{5}$$

Since the pressure losses consist of several components, the flow reduction coefficient F (or the effective discharge coefficient for the whole duct) is:

$$F = C_{d,eff} = \frac{1}{\sqrt{1 + \sum_{j=1}^{N} k_j}} \tag{6}$$

In the IMO Resolution MSC.245(83) the unity in the square root of Eq. (6) is included in the k-sum and considered to represent the pressure-losses due to the outlet of the duct, *Söding (2002)*.

The Resolution gives also a simple approach for calculation of the k-sum for a series of N successive openings:

$$\sum k = k_1 + \sum_{i=2}^{N} k_i \cdot \frac{S_1^2}{S_i^2}, \tag{7}$$

where S_i is the area of the opening i. Thus the pressure losses, weighted by the square of the relative area, are summed. This is a very simple approach and it does not take into account any effects from the stiffeners. *Pittaluga and Giannini (2006)* have observed from CFD calculations that the first opening in a duct has a more significant effect on the pressure losses than the subsequent ones, especially if the girders are close to each other.

3.4. Flooding Simulation

Similarly to the simplified method (section 3.2), also flooding simulation tools are based on Bernoulli's theorem, Eq. (3). However, the flow rates through the openings are integrated in time-domain and also the floating position is updated at each time step. In this study the NAPA Flooding Simulation tool has been used. Also the air compression and air flow can be calculated by using Bernoulli's equation for compressible flow. The details are given in *Ruponen (2007)*.

3.5. Several cross-flooding ducts

The Resolution MSC.245(83) also contains a very simplified approach for calculation of cross-flooding time if one pair of tanks is connected by several parallel cross-ducts. The total time t_{tot} is assessed by using the equation:

$$\frac{1}{t_{tot}} = \sum_{i=1}^{N_{duct}} \frac{1}{t_i}, \tag{8}$$

where t_i is the cross-flooding time, calculated for a single cross-duct and N_{duct} is the number of parallel ducts.

If there are many pairs of tanks, the cross-flooding time is the maximum of the times of all pairs. This is a rather simplified approach and it does not allow analysis of the situation during the cross-flooding process, e.g. at 60 s after the start of the flooding. For this purpose, only a time-domain flooding simulation can provide realistic results. In general the current regulations do not provide guidelines for calculation of simultaneous cross-flooding in several compartments.

3.6. Air compression

Restricted ventilation in a flooded tank can significantly slow down the cross-flooding time. The IMO Resolution MSC.245(83), *IMO (2007)* gives a very simple method for accounting the decreased flow rate in the cross-flooding duct due to air compression. The effective pressure loss coefficient for the cross-duct is determined as:

$$k_{eff} = k_w + k_a \cdot \frac{\rho_a}{\rho_w} \cdot \frac{S_w^2}{S_a^2}, \tag{9}$$

where ρ is density, S is the area of the duct or pipe and the subscripts a and w refer to air and water flows, respectively.

4. Determination of discharge coefficient for a cross-duct

4.1. Arrangement

The discharge coefficient of a typical cross-duct arrangement was evaluated by using CFD tools. The investigated design is exactly the same that was used in the experimental study in scale 1:3 by *Stening et al. (2011)*. Therefore the results are fully comparable. The case C2 with 5 girders and the stiffeners was selected. Each girder has two manholes (height 700 mm and width 400 mm). Thus the total cross-

flooding area is 0.491 m^2. The height of the stiffeners is 240 mm. The duct and the applied upstream (H_U) and downstream (H_D) water heights are illustrated in Fig. 2.

Based on the experimental results, the structural stiffeners inside the cross-duct and on the single girders increase the value of the discharge coefficient remarkably, *Stening et al. (2011)*. On the other hand, the influence of the inclination and the web-frame in the middle of the cross duct, were found to be negligible. The final conclusion was that the discharge coefficients of cross-ducts may be overestimated if the guidelines of MSC.245(83) are applied without properly considering and taking into account all the structures inside and geometrical properties of the cross-ducts. Therefore, such details were necessary to be properly implemented in the grid models for the CFD calculations. In addition, the scale effects and the influence of the inlet pressure height H_U could be studied.

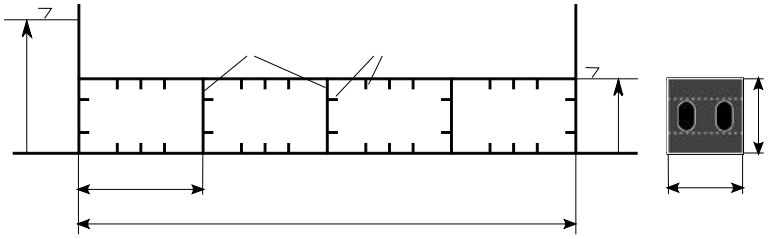

Fig. 2. Studied cross-duct arrangement (dimensions are meters in full-scale).

4.2. Computations

The applied software ISIS-CFD, developed by the CFD group of the Fluid Mechanics Laboratory and available as a part of the FINE™/Marine computing suite, is an incompressible unsteady Reynolds-averaged Navier-Stokes (URANS) method. The solver is based on the finite volume method to build the spatial discretisation of the transport equations. The unstructured discretisation is face-based, which means that cells with an arbitrary number of arbitrarily shaped faces are accepted. A detailed description of the solver is given by *Queutey and Visonneau (2007)*.

The computational geometry, presented in Fig. 3, is fully conformed to the experimental one, including the girders and the stiffeners. Only the symmetrical part of the cross-duct is modelled. The computational domain design and the boundary conditions are suited for the case, where the cross-duct is fully submerged. One additional box is added upstream of the duct in order to simulate the flow entrance. The upstream water elevation H_U, measured from the bottom of the cross-duct, is prescribed on the top face with the help of a pressure prescribed boundary condition. This corresponds to the darker face at the inlet in Fig. 3. Similarly, an additional box is added at the outlet with a prescribed pressure on the top face to simulate a prescribed downstream water elevation H_D for the outflow. Elsewhere on the surfaces wall-function boundary conditions are applied and the computations are carried out with the k-ω SST turbulence model.

The mesh is generated with the automatic HEXPRESS™ grid generator and contains about 11.7 million points. The wall-function approach was retained instead of the low-Reynolds number model due to the complexity of the geometry, see Fig. 3. On that grid the number of faces on the walls is about 0.8 million. To fulfil the $y^+ = 0.5$ constraint for a low-Reynolds approach, it would have been necessary to build a grid with about 50 million points which is out of the scope of the presented CFD study.

Grid dependence study has been performed for one case of the water elevation with a coarser grid having 6.7 million points and a finest grid with 16.3 million points. The 11.7 million points grid used for all the computations is the medium grid. For the three grids, it was checked that the normalized y^+ distance to the wall of the first layer of points is always lower than 60 even on the smallest elements (girders and stiffeners). For the case of the inlet water elevation H_U = 5 m, the relative computed

difference of the discharge coefficient to the finest grid is 3.2% for the coarser grid and 4.5% with the medium grid. This justifies the use of the medium grid for all the simulations since the uncertainty of the measured discharge coefficient is about 5%.

The effect of turbulence modelling has also been evaluated by using a non-linear explicit algebraic stress model (EASM), *Deng et al. (2005)*. This model takes into account the variation of production-to-dissipation rate ratio and includes a curvature correction. On the medium grid, the relative difference on the discharge coefficient obtained from the simulations using the k-ω SST turbulence model and the EASM turbulence model is about 4%. The EASM is 16% more expensive than classical isotropic two equations models. Hence the isotropic k-ω SST turbulence model was retained for all the simulations. Fig. 4 illustrates part of the surface grid in the middle region of the cross-duct and Fig. 5 shows the grid density in the same region from a Y-cut plane.

4.3. Results

4.3.1. Scale effects

A single computation in model scale (1:3) was performed for a fully immersed cross-duct with an inlet water height of H_U = 1.67 m and an outlet water height of H_D = 0.60 m, corresponding to the cross-duct height. The conditions were comparative to the experimental situation, *Stening et al. (2011)*. The computation was performed unsteady, starting from the water at rest with the pressure boundary conditions as mentioned previously. The time step was fixed to 0.001 s in order to prevent numerical instabilities, resulting from the initial conditions. Fig. 6 illustrates the distribution of the axial velocity in the Y-middle cut plane of Fig. 5 between the inlet and the outlet of the duct at t = 8 s, when the flow is fully developed. The flow enters the first manhole (located at X = 0 m) with a negative value of the vertical component of the velocity with respect to the prescribed pressure at the top of the inlet. This behaviour changes alternatively when the flow is passing through the successive manhole, which produces an oscillatory shape in the distribution of the axial velocity component.

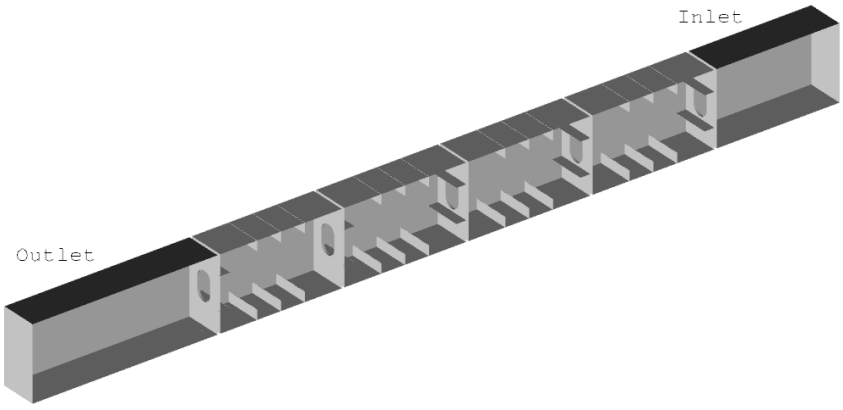

Fig. 3. Computational domain of the symmetric half of the cross-duct.

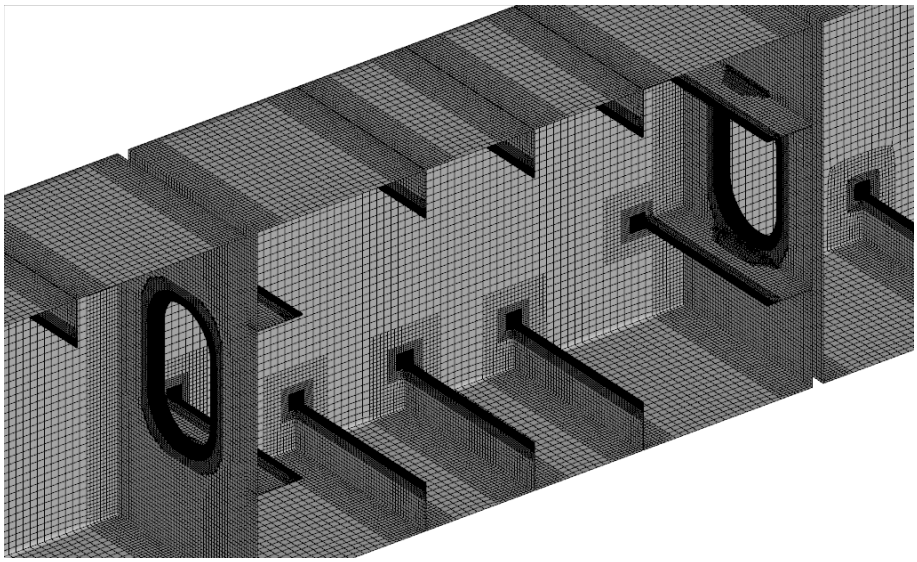

Fig. 4. Surface grid details.

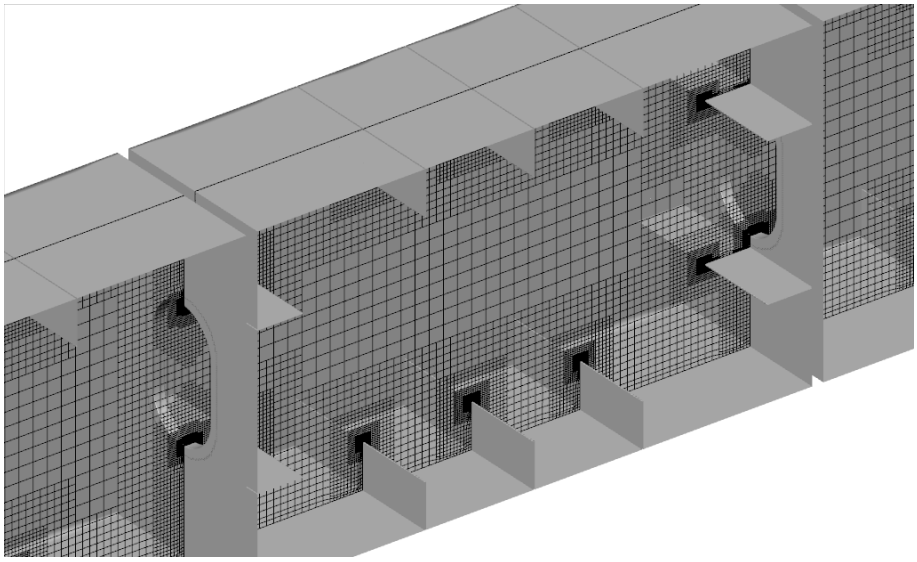

Fig. 5. Grid density details in a Y-cut plane.

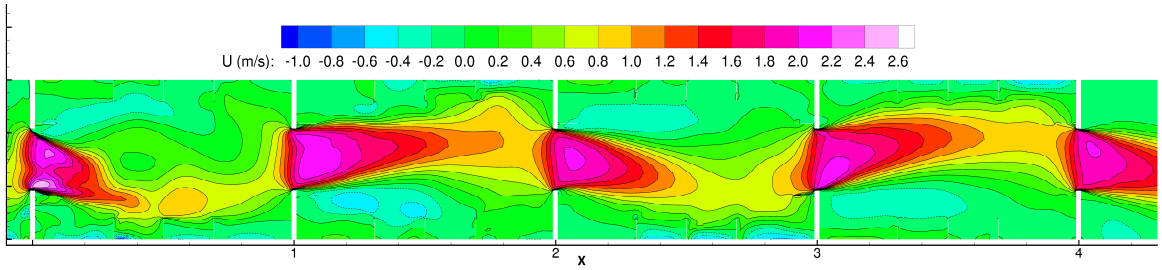

Fig. 6. Axial velocity component distribution in the Y-middle cut plane for the 1:3 scale computation.

Details showing the presence of the stiffeners between the second and the third girder in the duct are shown in Fig. 7. The action of the bottom and top stiffeners behind the manholes is supposed to decrease the intensity of the eddies around the jet in each compartment, *Stening et al. (2011)*.

The corresponding full-scale simulation domain uses the model-scale computational domain scaled by the factor 3. The full-scale computation is performed similarly to the computation at model scale,

except for the prescribed pressure values at inlet and outlet. For the full-scale simulation, it was possible to increase the time step up to 0.03 s without numerical instabilities once the flow was established.

Fig. 8 shows the distribution of the axial velocity component in the middle Y-cut plane when the flow is fully developed at t = 30 s. This is comparable with Fig. 6 for the model scale configuration. Except for the maximum speed (about 2 m/s at model scale and 4.5 m/s for the corresponding full-scale) and the shape of the jet behind the first manhole, the flow field behaves similarly between the second and the last openings.

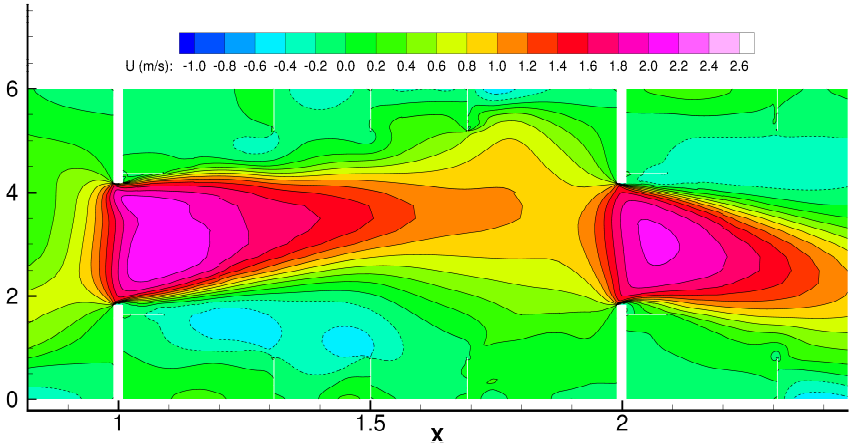

Fig. 7. Details of the axial velocity component distribution in the Y-middle cut plane for the 1:3 scale computation.

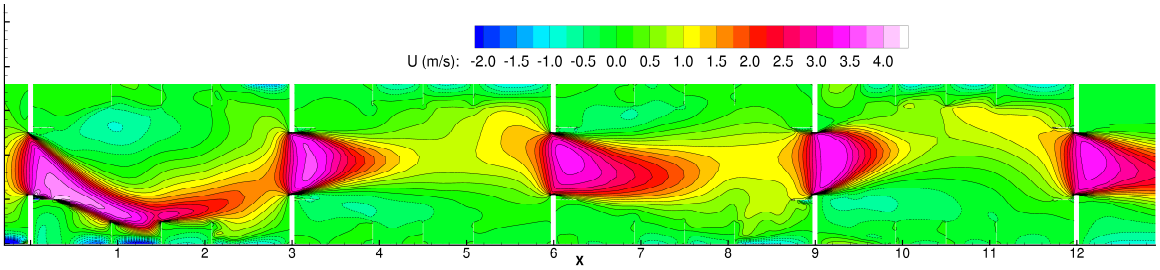

Fig. 8. Axial velocity component distribution in the Y-middle cut plane for the full-scale computation with inlet pressure height H_U = 5 m.

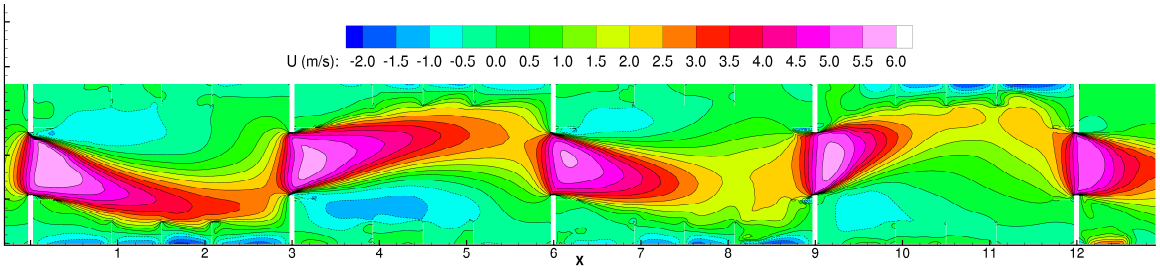

Fig. 9. Axial velocity component distribution in the Y-middle cut plane for the full-scale computation with inlet pressure height H_U = 10 m.

4.3.2. Higher inlet pressure at full-scale

In a realistic situation, the cross-duct is typically located from 5 m to 10 m below the sea water level. In order to assess the scale effect for a higher inlet water height, a second full-scale study was performed with H_U = 10 m. The instantaneous distribution of the axial velocity is presented in Fig. 9 in the previously used Y-cut plane. The main effect of the higher inlet pressure is the increase of the maximum speed by about 45%.

4.3.3. Discharge coefficient

The computed and measured flow rates and discharge coefficients are presented in Table 1. It appears that both computed discharge coefficients for full-scale simulations are similar within 3%, and that the model scale coefficient is between these two full-scale simulations with less than 2% of difference. The simulations predict the discharge coefficient in perfect agreement with the experimental results in model scale since the range of uncertainty of the measured discharge coefficient is considered to be about 5%.

The trend of the full-scale simulations indicates that no scale effect can be observed, at least for this unique downstream head to opening height ratio. However, considering the mean velocity speed corresponding to the computed mass flow rate, which is used to define the Reynolds number, is 1.53 m/s at model scale, 2.58 m/s at full-scale when H_U = 5 m, and 4.25 m/s at full-scale when H_U = 10 m. Consequently, the Reynolds number ratio between the full-scale (H_U = 5 m) and the model scale is about 5.0. Between the full-scale cases (H_U = 10 m and H_U = 5 m) the ratio is about 1.6. This relative low Reynolds number ratio explains the small differences of the computed discharge coefficient between the model scale and the full-scale simulations.

Table 1: Comparison of flow rates and discharge coefficients.

Case	Q **(m^3/s)**	C_d
model test *(Stening et al., 2011)*	0.043	0.338
model scale (CFD)	0.042	0.333
full-scale (CFD), H_U = 5 m	0.638	0.325
full-scale (CFD), H_U = 10 m	3.140	0.335

5. Pressure losses in air pipes

5.1. Case study

Evaluation of the pressure losses in air pipes is necessary in order to estimate the effect of restricted ventilation in the tank on the cross-flooding time. In the presented work, the pressure losses in air pipes were computed with the use of RANSE viscous flow model for two typical configurations with three selected values of overpressure in the vented tank. The investigated air pipes are illustrated in Fig. 10. Both pipes are of size DN250 with the inner diameter of 254 mm. The first pipe has two double-mitre bends and a free outlet. The second pipe design is straight with an air cap (Fig. 11) at the outlet. This kind of arrangement is typically used when it would be impractical to pull the pipeline all the way to the deck level. The air cap also prevents overflow from the sea to the tank.

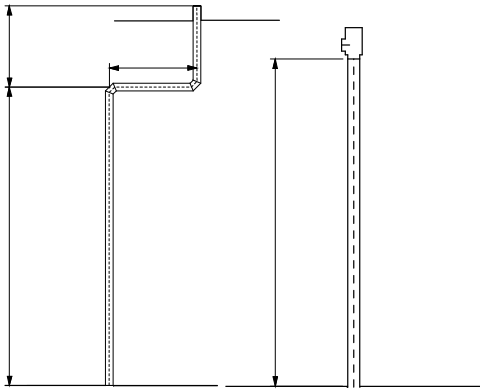

Fig. 10. Configurations of the air pipes.

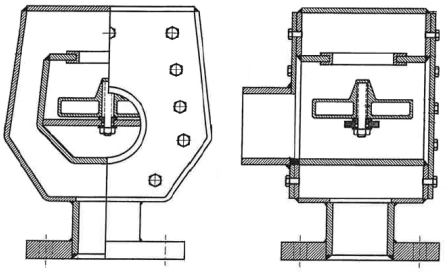

Fig. 11. Air cap at the outlet of air pipe 2.

5.2. CFD calculations

Calculations of the pressure loss coefficient for the air pipes were based on the assumption that the pressure changes in the vented compartment are relatively slow. Thus steady flow is a sufficient approximation of the actual flow. This flow condition can be achieved by enforcing constant overpressure at the pipe inlet and atmospheric pressure around the outlet. The computations were performed with the STAR CCM+ solver, using the k-ε turbulence model. Relatively coarse mesh was used near the boundaries (y^+ values of about 100); for that reason, the wall-function-type approach is used, in which it is assumed that the near-wall cell lies within the logarithmic region of the boundary layer. The flow was solved as an unsteady one, for the Case 1 the applied time step was 0.01 s and 0.005 s for the Case 2.

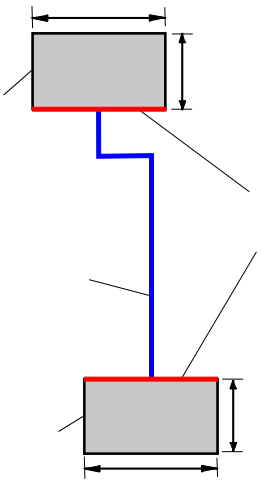

Fig. 12. Applied boundary conditions (Case 1).

Table 2: Dimensions of the inlet and outlet zones of the computational mesh.

	Height [mm]	Diameter [mm]
Inlet zone	2500	5460
Outlet zone	6500	5460

The losses at the pipe inlet and outlet contribute significantly to the total losses, so the flow in these regions has to be simulated directly. Therefore, the constant pressure has to be prescribed at some distance away from the inlet and the outlet. The regions of prescribed pressure are presented schematically in Fig. 12. The dimensions of the zones surrounding the inlet and outlet of the pipe are given in Table 2. The dimensions of the zones are identical for both studied configurations, but for the Case 2 the axis of the outlet zone is oriented horizontally, because the zone is fitted to the air cap at the pipe outlet.

In the calculations the air compressibility and gravity were taken into account and an ideal gas equation was used. The reference pressure is 101 325 Pa and the temperature is 300 K. Hexahedral unstructured mesh was used. The approximate number of cells is 800 000 for the air pipe Case 1 and 1 400 000 for the Case 2 (with the air cap at the outlet). The regular mesh dependency study was not carried out, however, the mesh for both cases was adapted after obtaining first results, so as to eliminate visible numerical diffusion. Sample sketches showing the meshes are presented in Fig. 13 and Fig. 14. For both air pipe configurations three values of overpressure at the inlet were considered: 1.0 kPa, 10 kPa and 20 kPa. These values roughly cover the expected range of overpressure occurring in the tank of a large passenger ship during the cross-flooding process.

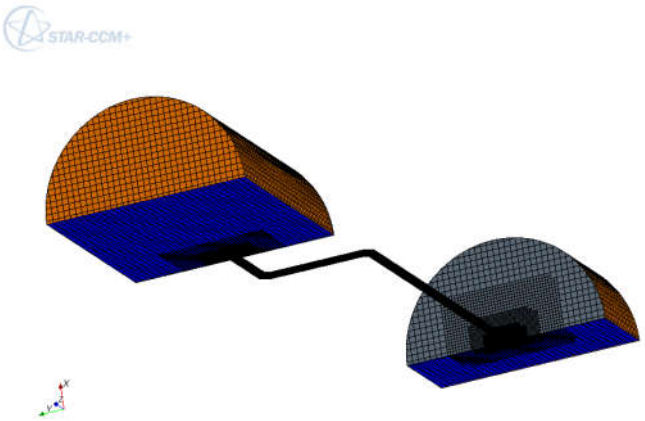

Fig. 13. Computational mesh for the Case 1, only half of the domain considered due to symmetry.

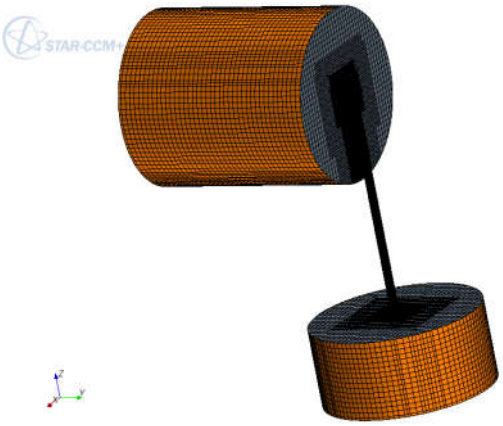

Fig. 14. Computational mesh for the Case 2.

5.3. Results

The effective discharge coefficient of the air pipe can be derived from the calculated mass flow $\dot{m}_{real}$ through the pipe:

$$C_{d,air} = \frac{\dot{m}_{real}}{\dot{m}_{theor}} \tag{10}$$

where $\dot{m}_{theor}$ is the maximum theoretical mass flow through the pipe, calculated by using Bernoulli's theorem, Eq. (3), with no pressure losses ($k_L = 0$).

The values of mass flow rate, discharge coefficient, pressure loss coefficient and maximum velocity for each case are summarized in Tables 3 and 4. The effective discharge coefficient is not very sensitive to the overpressure and the flow velocities. This indicates that the use of a constant value in cross-flooding analyses is well justified. It is also noteworthy that the calculated maximum flow velocities in the studied air pipes are very high: over 40 m/s, even with a moderate overpressure of 1.0 kPa (Case 2 with the air cap). With a high over-pressure of 20 kPa the maximum velocity is over 190 m/s, corresponding to a Mach number of about 0.56.

Examples of normalized pressure and velocity distributions near the inlet and outlet of both air pipe configurations with 10 kPa overpressure in the tank are presented in Fig. 15 and Fig. 16. The pressure was normalized by overpressure Δp at the inlet zone boundary and the velocity magnitude was normalized by the theoretical maximum speed in the air pipe at this overpressure without any losses, i.e. by $\sqrt{2\Delta p/\rho_0}$.

Table 3: Quantitative results for air pipe with free outlet (Case 1).

Overpressure [kPa]	**1.0**	**10**	**20**
Actual mass flow rate [kg/s]	1.427	4.741	6.793
Theoretical mass flow rate [kg/s]	2.485	7.859	11.115
Discharge coefficient $C_{d,air}$ [-]	0.574	0.603	0.611
Pressure loss coefficient k [-]	3.034	2.748	2.677
Maximum velocity [m/s]	37.8	124.7	176.5

Table 4: Quantitative results for air pipe with an air cap (Case 2).

Overpressure [kPa]	**1.0**	**10**	**20**
Actual mass flow rate [kg/s]	0.919	2.992	4.320
Theoretical mass flow rate [kg/s]	2.485	7.859	11.115
Discharge coefficient $C_{d,air}$ [-]	0.370	0.381	0.389
Pressure loss coefficient k [-]	7.321	6.901	6.619
Maximum velocity [m/s]	42.1	136.4	192.0

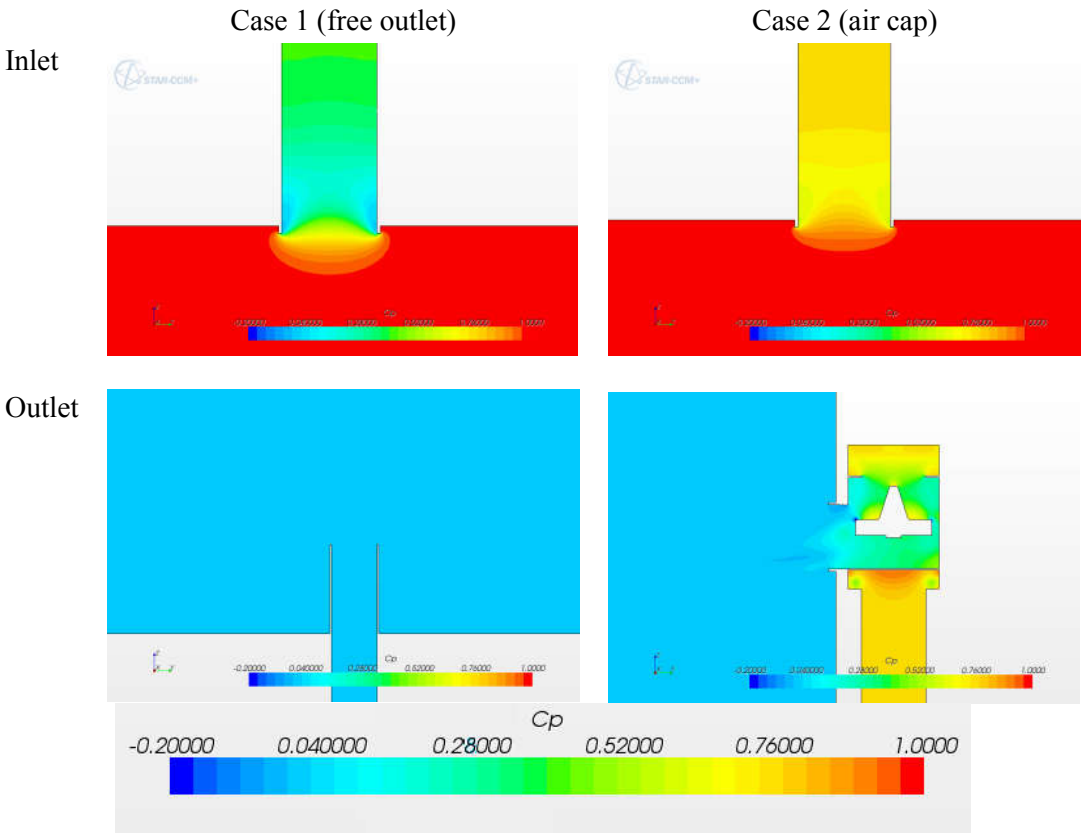

Fig. 15. Normalized pressure distribution in the inlet and outlet regions for overpressure 10 kPa.

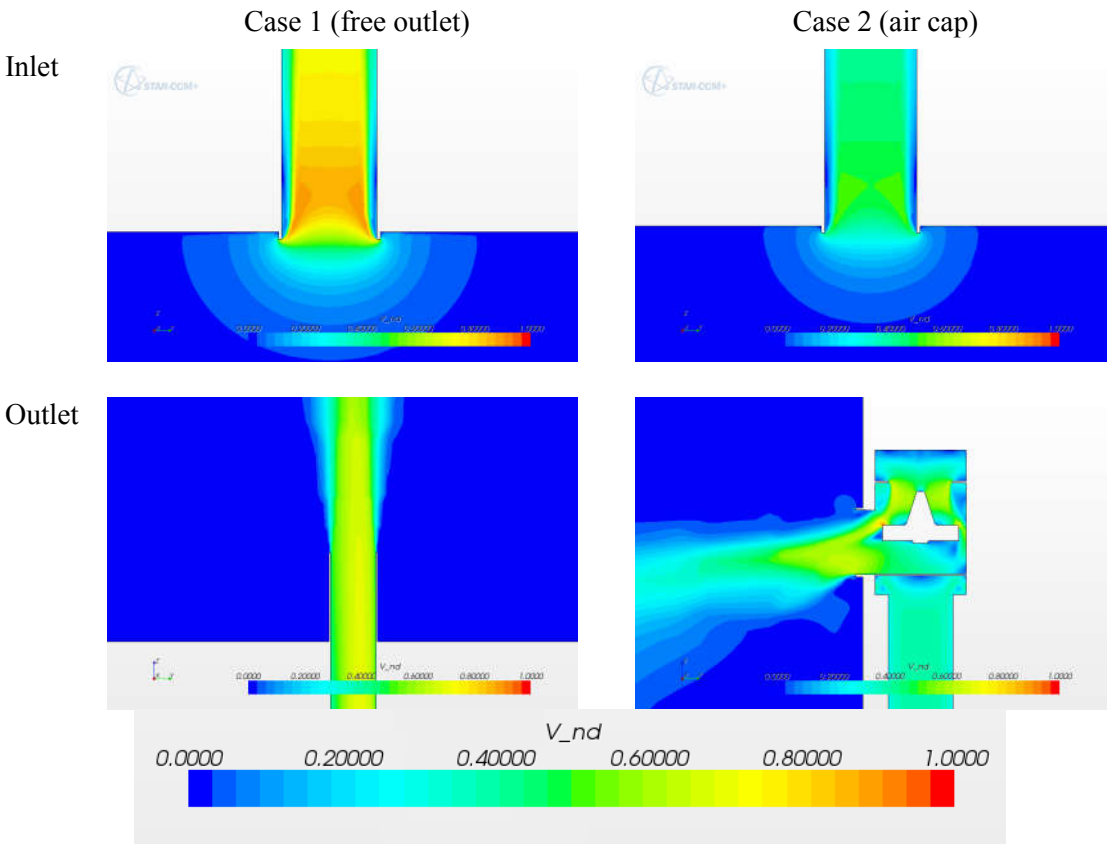

Fig. 16. Normalized velocity distribution in the inlet and outlet regions for overpressure 10 kPa.

5.4. Calculations according to MSC.245(83)

One of the goals of the study was to compare the CFD results with the simplified method, given in the IMO Resolution MSC.245(83). In this approach the total pressure loss coefficient is calculated by summing the k_i values for the particular elements of the pipe system (inlet, valves, bends etc.). Values for typical components are listed in the appendix of the Resolution. The calculation for the Case 1 is presented in Table 5, resulting in $\Sigma k = 3.52$. The CFD analysis gives Σk between 2.68 and 3.03, depending on the applied overpressure. Consequently, the simplified method over-estimates the pressure losses in the pipe by 16% – 31%. This can be due to the fact that the IMO Resolution is elaborated for water flows, for which the Reynolds number is usually smaller. Thus it results in higher pressure losses in general.

Table 5: Calculation of the *k*-sum for the pipe analyzed in Case 1.

Component	***k***
Inlet	0.43
Outlet	1.00
2 × 90° double mitre bend	0.88
Pipe friction (0.02×*L*/*D*)	1.21
***k*-sum**	**3.52**

The calculation method for frictional pressure losses in the pipe is based on the Darcy-Weisbach equation:

$$k_{friction} = f\frac{L}{D}, \tag{11}$$

where L is the pipe length and D is the inner diameter. In MSC.245(83) it is assumed that the dimensionless Darcy friction factor is constant $f = 0.02$. However, for turbulent flows, the friction factor can be solved iteratively from the Colebrook equation for a circular pipe, *Colebrook (1939)*:

$$\frac{1}{\sqrt{f}} = -2\log_{10}\left(\frac{\varepsilon}{3.7D} + \frac{2.51}{Rn\sqrt{f}}\right), \tag{12}$$

where ε is the pipe surface roughness and Rn is Reynolds number. The Darcy friction factor for the studied DN250 pipe with the assumed surface roughness $\varepsilon = 0.1$ mm is presented as a function of Reynolds number in Fig. 17. For high Reynolds numbers the coefficient is smaller than assumed in MSC.245(83). This explains partly why the CFD analysis results in notably smaller pressure losses than the simplified calculation method.

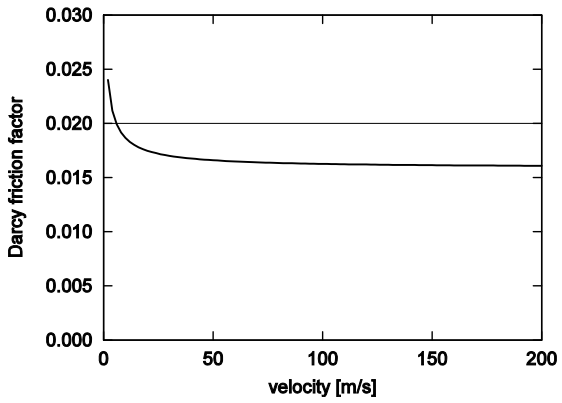

Fig. 17. Darcy friction factor for DN250 pipe.

6. Cross-flooding case study

6.1. Arrangement and damage scenario

A comprehensive case study was performed in order to assess the effect of different methods for determination of the discharge coefficients on the cross-flooding time. A modern large cruise ship design, developed by STX Finland for the FLOODSTAND project (*Jalonen et al., 2010*), was used. A two-compartment damage scenario was selected to represent a situation with large heeling due to the asymmetric distribution of the floodwater. The flooding on the upper decks is assumed to be instantaneous. As a result, the initial heeling angle before the cross-flooding is 5.2°. The damage scenario is illustrated in Fig. 18. The total volume for cross flooding water, W in Eq. (1), is about 389 m^3. The double bottom tanks in both compartments have almost equivalent size and geometry.

The empty tanks in the double bottom are connected by two parallel 18 m long cross-ducts with two manholes in the girders. This is the longest duct design (Case C6) that has been tested in model-scale 1:3, *Stening et al. (2011)*. The girders and stiffeners are arranged similarly to the Case C2 that was used in the CFD analysis in chapter 4. Since the web frame in the middle of the tested duct did not have a notable effect on the discharge coefficient, the results of the model tests are assumed to be applicable also to parallel ducts.

The tanks are ventilated through air pipes (Case 1 in chapter 5), containing two 90° double mitre bends and free outlet to the atmosphere without any valve or an air cap. The area of the air pipe is 4.9% of the total area of the cross-flooding openings. Consequently, according to MSC.245(83) the air compressibility needs to be accounted.

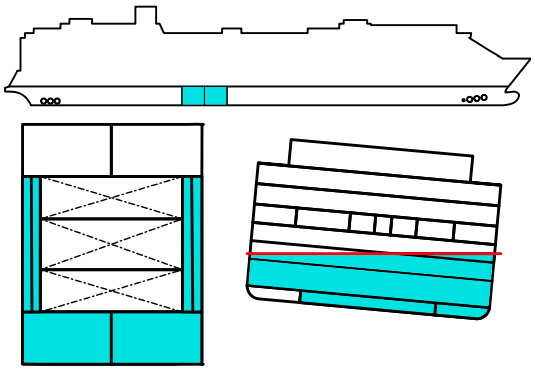

Fig. 18. Damage scenario before cross-flooding.

6.2. Calculations

Calculations for the cross-flooding time were performed with the NAPA software, using both the time-domain flooding simulation feature (*Ruponen, 2007*) and the simplified method of MSC.245(83), Eq. (1). In the simulation the actual air compression inside the tanks was calculated. The applied time step was 0.1 s. In the simplified approach the effective discharge coefficient of the cross-duct was modified according to Eq. (9), based on the pressure losses in the air pipe. Comparative calculations were also performed with the assumption of full ventilation in the tanks.

The applied discharge coefficients for the cross-ducts and the air pipes are presented in Table 6. First the regression equation for this type of duct (*Pittaluga and Giannini, 2006*) is used to calculate the pressure loss coefficient for each space between two adjacent girders:

$$k_i = 0.0424L_i^3 - 0.3593L_i^2 + 1.1401L_i - 0.356, \quad 1 \le L_i \le 4, \tag{13}$$

where L_i is the distance between two adjacent girders in meters. In this case L_i = 3.0 m. The second approach uses the Eq. (7) and a rough estimation of C_d = 0.6 for each manhole. Consequently, the

pressure loss coefficient for each girder is k_i = 1.778. With both methods, the discharge coefficient is calculated by using Eq. (6), where the effect of the outlet (k_i = 1) is accounted. In the third approach the experimental result from the model test (*Stening et al., 2011)* is used.

The air compression effect in the simplified method, Eq. (1), was taken into account according to the Eq. (9). The applied reference density of air in atmospheric pressure is 1.177 kg/m^3 and water density is 1025 kg/m^3. The resulting additional pressure-loss coefficient is presented in Fig. 19 as a function of the air pipe discharge coefficient.

Table 6: Discharge coefficients for the cross-duct and air pipe.

Item	**Calculation method**	C_d
Cross-duct	MSC.245(83), *Pittaluga and Giannini (2006)*	0.382
Cross-duct	Subsequent manholes, Eq. (7)	0.273
Cross-duct	Model tests, *Stening et al. (2011)*	0.287
Air pipe	CFD	0.580
Air pipe	MSC.245(83)	0.533

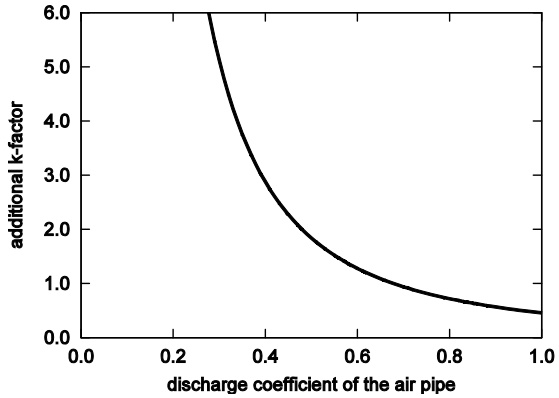

Fig. 19. Additional pressure loss coefficient k according to Eq. (9) for the studied cross-duct due to limited ventilation level in the tank.

6.3. Results

The cross-flooding times, calculated by using the simple calculation method of MSC.245(83), are presented in Table 7. The corresponding results of time-domain flooding simulations are given in Table 8. The regression Eq. (13) over-estimates the discharge coefficient by 39%, when compared to the measured value. Consequently, the calculated cross-flooding time is about 25% faster. For comparison, a cross-flooding pipe with the cross-section fitting the manhole would have a much larger discharge coefficient of 0.683 when the pipe friction is calculated with Eq. (11) and Darcy friction factor 0.02 (as in *IMO, 2007*).

Air compression in the tank clearly delays the cross-flooding time by 6% – 11%. Although the difference in the applied C_d for the air pipes is notable (about 9%), the effect on the time is much smaller (less than 2%). This suggests that the simplified approach for accounting the pressure losses in the air pipes might be accurate enough for many practical applications. However, as shown in Fig. 20, for smaller C_d values of the air pipe, the effect of small difference can be much larger.

The simplified method for calculation of the cross-flooding time provides very similar results to the time-domain flooding simulation. The maximum difference is only about 2%. The maximum simulated overpressure in the tanks is about 10 kPa. An example of the time history of simulated air overpressure in the tank is shown in Fig. 20. Eventually the whole tank is filled up and thus the air pressure does not decrease back to the atmospheric pressure. The volume of floodwater in this tank increases almost linearly, Fig. 21. This partly explains the good correlation between the simplified method of Eq. (1) and time-domain simulation.

Table 7: Cross-flooding times [s] with the simple calculation method, Eq. (1).

Calculation method for cross-duct C_d:	**full ventilation**	**C_d for air pipes:**	
		MSC.245(83)	**CFD**
MSC.245(83), *Pittaluga and Giannini (2006)*	46.0	51.1	50.3
MSC.245(83), Eq. (7)	64.4	68.1	67.6
Model test, *Stening et al. (2011)*	61.2	65.1	64.6

Table 8: Cross-flooding times [s] with the time-domain flooding simulation.

Calculation method for cross-duct C_d:	**full ventilation**	**C_d for air pipes:**	
		MSC.245(83)	**CFD**
MSC.245(83), *Pittaluga and Giannini (2006)*	46.4	52.1	51.1
MSC.245(83), Eq. (7)	64.8	68.6	67.9
Model test, *Stening et al. (2011)*	61.7	65.7	65.0

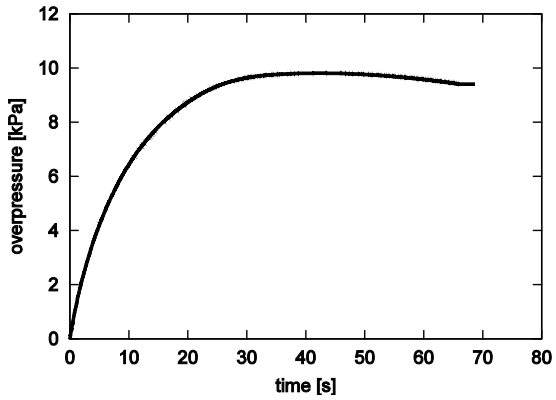

Fig. 20. Example of simulated overpressure in the tank on the undamaged side.

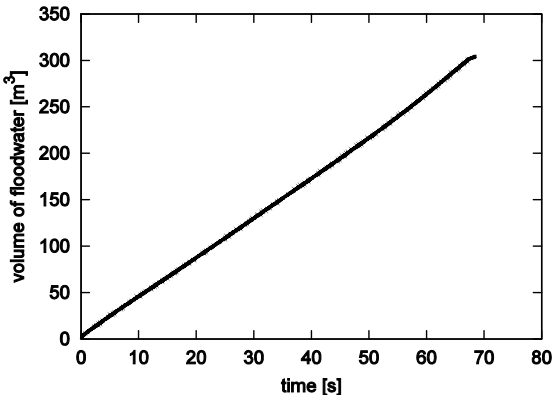

Fig. 21. Example of volume of floodwater in the tank on the undamaged side.

7. Conclusions

Determination of the discharge coefficient for the cross-flooding ducts and air pipes is a challenging task for the ship designer. The regulations allow different methods that may produce contradicting results. The presented calculations have provided new insight to deal with this problem.

In the present study, the CFD analysis for a typical cross-duct design resulted in a discharge coefficient that corresponds very well with the available experimental data. Moreover, the scale effects for comparative computations in the model scale (1:3) were minimal, thus providing further support for the conclusions from the experiments*, Stening et al. (2011)*. Moreover, the pressure height at the inlet of the duct did not affect discharge coefficient. This supports the widely used assumption that the discharge coefficient can be taken as a constant during the flooding.

In the presented case study the use of the regression Eq. (13) by *Pittaluga and Giannini (2006)* for determination of the discharge coefficient for the whole cross-duct results in significant under-estimation of the cross-flooding time. Instead, applying $C_d = 0.6$ and Eq. (7) for each opening in the girders provided very similar results to the model tests analysis and the cross-flooding time is only slightly over-estimated. Besides, the major benefit of Eq. (7) is that it can be applied to cross-duct designs, where the number and size of the manholes varies between the girders.

CFD analysis was used also to determine discharge coefficients for two typical air pipe designs. The applied overpressure in the tank had only a minimal effect on the discharge coefficient of the air pipe in both studied configurations. Based on this, it seems to be justified to use a constant C_d for an air pipe in the calculation of cross-flooding time. Moreover, the CFD analysis pointed out that the flow velocities in the air pipes can be very high, up to 200 m/s. The Colebrook equation can be used for more accurate estimation of frictional pressure losses. Yet in the case study the differences in the air pipe pressure losses had only a minimal effect on the cross-flooding time. However, the result may not be generalized. Thus Eq. (9) should be used to analyze the sensitivity to small errors if the simplified method of MSC.245(83) is used to assess the pressure losses in the air pipe.

MSC.245(83) also suggests that full ventilation level can be assumed if the area ratio between the ventilation pipe and cross-duct is larger than 10%. This is very questionable since it does not take into account the pressure losses in the air pipe (length of the pipe, bends, valves, etc.). It is highly recommended to include the air compressibility in all cross-flooding analyses unless the ventilation is arranged through extremely large pipes with very small pressure losses.

In the studied case both the simple method of MSC.245(83), Eq. (1), and the time-domain flooding simulation result in almost equivalent cross-flooding times. This is partly explained by the fact that the cross-flooding takes place purely below the double bottom. Thus the decrease of the effective pressure head during the flooding is rather small, and consequently, the flow rate is almost constant. Moreover, the simplified method for accounting counter air pressure, Eq. (9), seems to correspond well with the time-domain simulation. However, the results may not be extended to very different flooding cases like large U-shaped voids with much higher over-pressures due to restricted ventilation level in the tanks.

It should also be remembered that the regulation is based on the assumption that the damaged rooms are instantly flooded. This is not realistic, especially if the damage hole is small. Furthermore, in the damaged side the air compression will actually slow down the flooding from the sea. In reality, the cross-flooding starts as soon as the water level reaches the duct. This can have a very significant reduction in the maximum heeling angle during the flooding, *Ruponen and Routi (2007)*.

The simultaneous cross-flooding in several compartments needs to be studied further. In the presented case study the volumes and cross-duct arrangements were practically identical. Thus the conclusions might not be valid for a case, where the cross-flooding times of the tanks are significantly different.

Currently time-domain simulation is the only method for proper assessment of this kind of situation, especially during the flooding process, for example at 60 s after the commencement of flooding.

Based on this study, it seems to be justified to use the simplified approach of Eq. (7) for determination of the discharge coefficient for the cross-duct. However, CFD analysis or large scale model tests may be needed for exceptional arrangements. Time-domain flooding simulation and air compression is needed in the cases, where the cross-flooding involves serial connections or air compression is expected to be very significant. However, more investigations with different cross-duct and air pipe configurations are still needed in order to derive more comprehensive conclusions and recommendations.

Acknowledgment

The research leading to these results has received funding from the European Community's Seventh Framework Programme (FP7/2007-2013) under grant agreement no. 218532 (project FLOODSTAND). The financial support is gratefully appreciated. The authors would also like to thank Ms. Anna-Lea Routi from STX Finland for her help in the planning of the test cases. Mr. Mikael Stening and Dr. Juha Järvelä are thanked for providing the experimental results. Any opinions expressed in this paper are those of the authors.

References

Colebrook, C.F., 1939. Turbulent flow in pipes, with particular reference to the transition region between smooth and rough pipe laws, Journal of the Institution of Civil Engineers, vol II 1938-1939, 133-156.

Deng, G.B., Queutey, P., Visonneau, M. 2005. Three-Dimensional Flow Computation with Reynolds Stress and Algebraic Stress Models. Engineering Turbulence Modelling and Experiments 6, 389-398. W. Rodi and M. Mulas, editors. Elsevier Ltd.

IMO, 1973. Resolution A.266(VIII): Recommendation on a Standard Method for Establishing Compliance with the Requirements for Cross-Flooding Arrangements in Passenger Ships. London, UK.

IMO, 2007. Resolution MSC.245(83): Recommendation on a Standard Method for Evaluating Cross-Flooding Arrangements. London, UK.

IMO, 2008. Resolution MSC.281(85): Explanatory Notes to the SOLAS Chapter II-1 Subdivision and Damage Stability Regulations. London, UK.

IMO, 2010. SLF53/INF.6: Research on the application of computational fluid dynamics (CFD) to an alternative to the evaluation method for cross-flooding arrangements, submitted by Japan. London, UK.

Jalonen, R., Jasionowski, A., Ruponen, P., Mery, N., Papanikolaou, A., Routi, A.-L. 2010. FLOODSTAND – Integrated Flooding Control and Standard for Stability and Crises Management, Proceedings of the 11th International Ship Stability Workshop, Wageningen, The Netherlands, 159-165.

Pawlowski, M. 2004. Subdivision and damage stability of ships, Euro-MTEC book series, Foundation for the Promotion of Maritime Industry, Gdansk, ISBN 83-919488-6-2, 311 p.

Peters, A.J., Galloway, M., Minnick, P.V., 2003. Cross-Flooding Design Using Simulations. Proceedings of the 8th International Conference on Stability of Ships and Ocean Vehicles, Madrid, Spain, 743-755.

Pittaluga, C., Giannini, M., 2006. Pressure Losses Estimation for Structural Double Bottom by CFD Technique. CETENA Technical Report, Italy.

Queutey, P., Visonneau, M., 2007. An Interface Capturing Method for Free-Surface Hydrodynamic Flows, Computers & Fluids 36, 1481-1510.

Ruponen, P., Routi, A.-L., 2007. Time-Domain Simulation of Cross-Flooding for Air Pipe Dimensioning. Proceedings of the 9th International Ship Stability Workshop, Hamburg, Germany.

Ruponen, P., 2007. Progressive Flooding of a Damaged Passenger Ship, Doctoral dissertation, Helsinki University of Technology, TKK Dissertations 94, Espoo, Finland.

Söding, H., 2002. Flow computations for ship safety problems. Ocean Engineering 29, 721-738.

Solda, G.S., 1961. Equalisation of Unsymmetrical Flooding. Transactions of Royal Institute of Naval Architects 103, 219-225.

Stening, M., Järvelä, J., Ruponen, P., Jalonen, R., 2011. Determination of discharge coefficients for a cross-flooding duct, Ocean Engineering 38, 570-578.

Vassalos, D., 2009. Risk Based Ship Design, Risk Based Ship Design (ed. A. Papanikolaou), Springer Verlag, pp. 17-96.